



Article

Identification of Isoform-Selective Ligands for the Middle Domain of Heat Shock Protein 90 (Hsp90)

Oi Wei Mak ¹, Raina Chand ¹, Jóhannes Reynisson ^{1,2,*} and Ivanhoe K. H. Leung ^{1,3,*}

¹ School of Chemical Sciences, The University of Auckland, Private Bag 92019, Victoria Street West, Auckland 1142, New Zealand; omak089@aucklanduni.ac.nz (O.W.M.); rcha387@aucklanduni.ac.nz (R.C.)

² School of Pharmacy and Bioengineering, Hornbeam Building, Keele University, Keele, Staffordshire ST5 5BG, UK

³ Maurice Wilkins Centre for Molecular Biodiscovery, The University of Auckland, Private Bag 92019, Victoria Street West, Auckland 1142, New Zealand

* Correspondence: j.reynisson@keele.ac.uk (J.R.); i.leung@auckland.ac.nz (I.K.H.L.); Tel.: +44-1782-733-985 (J.R.); +64-9-923-1102 (I.K.H.L.)

Received: 12 September 2019; Accepted: 23 October 2019; Published: 26 October 2019



Abstract: The molecular chaperone heat shock protein 90 (Hsp90) is a current inhibition target for the treatment of diseases, including cancer. In humans, there are two major cytosolic isoforms of Hsp90 (Hsp90 α and Hsp90 β). Hsp90 α is inducible and Hsp90 β is constitutively expressed. Most Hsp90 inhibitors are pan-inhibitors that target both cytosolic isoforms of Hsp90. The development of isoform-selective inhibitors of Hsp90 may enable better clinical outcomes. Herein, by using virtual screening and binding studies, we report our work in the identification and characterisation of novel isoform-selective ligands for the middle domain of Hsp90 β . Our results pave the way for further development of isoform-selective Hsp90 inhibitors.

Keywords: Hsp90; virtual screening; intrinsic tryptophan fluorescence; ligand binding; isoform-selective

1. Introduction

Heat shock protein 90 (Hsp90) is a class of 90 kDa dimeric chaperone proteins from the heat shock protein family [1–11]. Members of the Hsp90 family are highly conserved and can be found in almost all organisms (except for archaea) [12–14]. The main function of Hsp90 is to maintain the proper folding of proteins within the cell [1–11]. Its specific tasks include the assistance of folding of the nascent polypeptide chains, the stabilisation of proteins (in particularly during heat shock or other stress conditions), and catalysing the refolding of denatured proteins [1–11]. Due to the central role Hsp90 plays in protein folding and stabilisation, the protein is involved in many important cellular processes. These include (but are not limited to) the regulation of cellular homeostasis, cell cycle control, signal transduction, and cytoprotection [1–11].

Structurally, each Hsp90 monomer comprises three domains [4,6,9–11], which are termed the N-terminal domain (NTD), middle domain (MD), and C-terminal domain (CTD). The NTD is joined with the MD through a flexible linker, which is named the charged region. The NTD binds and catalyses the hydrolysis of adenosine triphosphate (ATP), which induces conformational change that is essential to the chaperone function of Hsp90 [15,16]. The CTD contains the homodimerisation site [17,18], whilst the MD is responsible for client protein binding [19,20]. The MD also modulates the ATPase activity of the NTD through interactions with the γ -phosphate moiety of ATP [19,20]. The activity of Hsp90 is mediated by a number of co-chaperones [21,22]. All three domains are involved in the binding of different co-chaperones [21,22].

In humans, there are two major cytosolic isoforms of Hsp90, which are Hsp90 α and Hsp90 β (Table S1) [23]. There are inherent differences between the cellular processes that the two isoforms

are involved in. Hsp90 β is constitutively expressed and it is associated with long-term processes such as cellular adaptation [23–26]. In contrast, Hsp90 α is involved in processes that require fast response, presumably because it is inducible and shows different client protein preferences under stress conditions [23–27].

Hsp90 is a current inhibition target for the treatment of diseases including cancer. This can be attributed to Hsp90's ability to maintain and regulate oncoproteins [28,29], as well as those proteins that aid the initiation and progression of tumours [5,30]. For example, overexpression of Hsp90 α is often found in acute and chronic tumours (but not benign tumours), and Hsp90 β has been implied in multidrug resistance in chronic tumours [23]. There is, therefore, a great anticipation towards the development of Hsp90 inhibitors with cancer therapeutic potential. For example, the inhibition of Hsp90 has been shown to lead to cell cycle arrest and apoptosis of cancerous cells [31]. The inhibition of Hsp90 may also help overcome resistance in chemotherapy [32–34].

Numerous inhibitors of Hsp90 have been discovered in the last 15 years [35–47]. Most of them target binding sites at the NTD and CTD. For example, geldanamycin [48,49], 17-N-allylamino-17-demethoxygeldanamycin [50], and ganetespib (also known as STA-9090) [51,52] target the ATP binding pocket at the NTD, and novobiocin was found to bind the CTD of Hsp90 [53]. In spite of the discovery of numerous inhibitors that target the NTD and CTD, there are only few studies on the inhibition of MD [54,55]. It is also worth noting that all 17 small molecule Hsp90 inhibitors that have entered clinical trials to date target the NTD of both isoforms of Hsp90 [35–47]. Only a handful of isoform-selective Hsp90 inhibitors have been reported [55–62].

We are interested in the development of novel Hsp90 inhibitors. In particular, the isoform-selective Hsp90 inhibitors are of importance because they may give better clinical outcomes than pan-Hsp90 inhibitors [63–65]. In addition, isoform-selective inhibitors will also enable studies on the roles of the different Hsp90 isoforms without resorting to genetic manipulations, which are often more invasive. The MD of Hsp90 is of particular interest because the possibility exists to develop isoform-specific Hsp90 binders [55,56] due to the inherent differences in client protein selectivity of the two isoforms especially during stress conditions [27]. Herein, we report our work in the application of virtual high-throughput screening and binding experiments, a strategy that we have previously used to discover Hsp90 NTD inhibitors [66], to identify novel isoform-selective ligands for MD of Hsp90 β . Our report provides novel scaffolds for future development of isoform-selective Hsp90 β MD inhibitors.

2. Results and Discussion

We first investigated potential binding pockets on the MD of Hsp90 β that could be targeted by small-molecule ligands. Unlike the NTD and CTD of Hsp90, the MD does not have a well-defined binding site for small molecule ligands. We therefore performed blind docking experiments to predict the most probable binding site for small molecule ligands [67,68]. Gambogic acid, an isoform-selective inhibitor of the MD of Hsp90 β [55], was used as the model ligand, and the crystal structure of the MD of human Hsp90 β (PDB ID: 3PRY, resolution 2.28 Å) was used as the target. Eighty-seven different potential binding sites on Hsp90 β were evaluated by using a consensus scoring approach [69,70] that is based on four different scoring functions, GoldScore (GS) [71], ChemScore (CS) [72,73], piecewise linear potential (ChemPLP) [74], and Astex Statistical Potential (ASP) [75] (Table S2). Our docking results revealed a site within a 10 Å radius centring around the oxygen atom on the sidechain of Asp-367 ($x = 8.806$, $y = 23.993$, $z = 27.785$; Figure S1) as the most probable pocket that could be targeted by small molecules. The binding pocket that we identified is consistent with previous molecular modelling work that suggested the region consisting of residues 350 to 436 as the potential binding site for gambogic acid [55].

High-throughput virtual screening was then conducted against the identified binding site. In total, 9051 molecular entities were downloaded from the natural product library from the InterBioScreen Ltd collection. Ten docking runs were carried out for each ligand with 30% search efficiency. From the consensus scoring, all ligands with low CS (<15.0), GS (<51.0), ChemPLP (<55.0), and ASP (<25.2)

scores, as well as those with limited hydrogen bonding ($HB < 1$) were eliminated in the initial screen. 913 candidates remained, and they were screened again with 100% default search efficiency and 50 genetic algorithm (GA) runs. The candidates with low scores on CS (<20.0), GS (<60.0), ChemPLP (<60.0), ASP (<25.0), and HB (<1) were then filtered out, resulting in 152 compounds. The 152 candidate compounds all have docking scores higher than the score that we obtained by docking gambogic acid to Hsp90 β . Visual inspection was then conducted for consensus of the best predicted configuration of the ligands between each scoring function. Ligands that showed implausible configurations, i.e., those that are strained, with lipophilic moieties pointing towards aqueous environment, and those that contain undesirable moieties (e.g., those that are linked to cell toxicity and chemical reactivity), were eliminated.

As a result of virtual screening, 24 hit compounds (Figure 1 and Table S3) were selected for further experimental testing against recombinant human Hsp90 α MD (residues 294 to 554, Table S4) and human Hsp90 β MD (residues 286 to 546, Table S5). As there are tryptophan residues located within the defined binding pocket in both Hsp90 α MD and Hsp90 β MD, intrinsic tryptophan fluorescence quenching experiment was used to screen the binding of our virtual hits to the proteins. Initial screening experiments were conducted by using 20 μM of Hsp90 α/β MD and 1 mM of compounds. Molecules that gave less than 40% fluorescence quenching were eliminated. Our results revealed that eight compounds (**5**, **8**, **9**, **12**, **17**, **22**, **24**) bind to both Hsp90 α MD and Hsp90 β MD. In addition, one compound (**10**) was found to induce significant quenching ($\sim 90\%$) of Hsp90 β MD but not with Hsp90 α MD ($\sim 20\%$) (Figure 1, Table S6, and Figure S2).

We then focussed on studying the binding of our compounds (**5**, **8**, **9**, **10**, **12**, **17**, **22**, **24**) to both Hsp90 α MD and Hsp90 β MD. Titration experiments were performed to quantify the binding affinity (dissociation constant, K_D) to Hsp90 α MD and Hsp90 β MD (Table 1 and Figures S3–S10). The K_D values of gambogic acid were also measured as control (Table 1 and Figure S11). Our results show that compounds **5**, **9**, **10**, **12**, **17**, and **24** bind stronger to Hsp90 β MD than to Hsp90 α MD. The strongest binder was **12**, which binds to Hsp90 β MD with a K_D value of $< 20 \mu\text{M}$, and a K_D value of $92 \pm 0.8 \mu\text{M}$ to Hsp90 α MD. The seven-fold preference for the β -isoform is similar to gambogic acid, which has a K_D value of $195 \pm 5 \mu\text{M}$ with Hsp90 α MD, and a K_D value of $33 \pm 2 \mu\text{M}$ with Hsp90 β MD. Our K_D values for gambogic acid are in agreement with previous studies (~ 10 -fold preference) [55]. The selectivity for the β -isoform (over α -isoforms) was progressively less for weaker binders. For example, compound **9**, which binds Hsp90 β MD with a K_D value of $57 \pm 1 \mu\text{M}$, only shows a 5-fold selectivity for Hsp90 β MD. The selectivity of compound **5**, a structure analogue of compound **9** that binds Hsp90 β MD with a K_D of $136 \pm 1 \mu\text{M}$, was found to be ~ 3 -fold. Compounds **10**, **17**, and **24** (which bind Hsp90 β MD with K_D values $> 100 \mu\text{M}$) only show ~ 2 - to 3-fold preference for the β -isoform. Compounds **8** and **22**, which bind Hsp90 β MD with $K_D > 500 \mu\text{M}$, actually have a slight preference for Hsp90 α MD, with K_D values of $284 \pm 4 \mu\text{M}$ and $459 \pm 7 \mu\text{M}$, respectively.

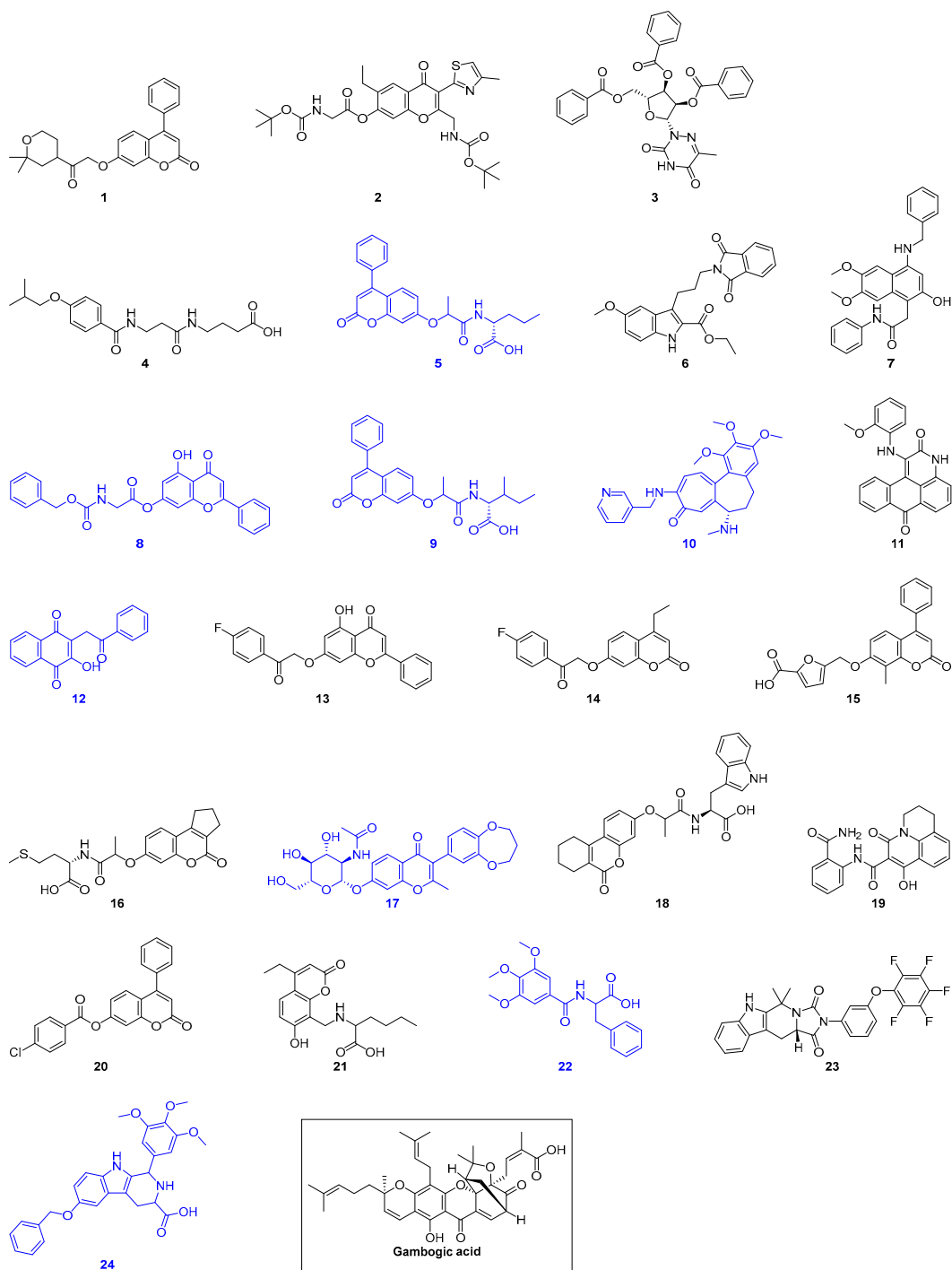


Figure 1. Structures of the 24 virtual hits and gambogic acid (a reported Hsp90 MD inhibitor). Blue indicates compounds that show binding to Hsp90 α/β MD as monitored by intrinsic tryptophan fluorescence spectroscopy.

Table 1. Binding affinity (K_D) of our compounds to Hsp90 α/β MD. Gambogic acid was used as a control.

Compound	K_D to Hsp90 α MD/ μ M	K_D to Hsp90 β MD/ μ M
5	470 \pm 2	136 \pm 1
8	284 \pm 4	500
9	299 \pm 3	57 \pm 1
10	>500	164 \pm 2
12	92 \pm 0.8	<20
17	506 \pm 4	285 \pm 8
22	459 \pm 7	>500
24	661 \pm 3	265 \pm 4
Gambogic acid	195 \pm 5	33 \pm 2

Molecular docking of compounds **5**, **8**, **9**, **10**, **12**, **17**, **22**, and **24** were then conducted to predict the binding modes and relative energies of the compounds to the two isoforms of Hsp90 MD. The same four scoring functions (ChemPLP, GS, CS, and ASP) were used. For example, with compound **12**, our docking results showed that the compounds bind to different part of the equivalent binding site (10 Å radius from residue Glu-375 for Hsp90 α MD (PDB id: 3Q6M; $x = -1.652$, $y = -64.237$, $z = 27.08$) and residue Asp-367 for Hsp90 β MD; Figure S1) on the two isoforms (Figure 2). The scale of the fitness scores derived from the docking algorithms showed that all eight compounds have higher scores and more hydrogen bonding interactions towards the binding pocket of Hsp90 β MD when compared to the docking results to Hsp90 α -MD (Table S7; Figure 3 and Figures S12–S18). For example, for compound **12**, the GS scoring function suggested that it does not have any hydrogen bonding interactions with the neighbouring amino acid residues of Hsp90 α MD, but it forms three different hydrogen bonds with Hsp90 β MD (Figure 3). The ligand binding positions that are generated by the search algorithm component of molecular docking showed that the most likely binding pose of each compound has the better fitness for the β -isoform than the α -isoform. These computational results correlate well with the experimental trend of K_D values for compounds **5**, **9**, **10**, **12**, **17**, and **24** from the binding assay. For compounds **8** and **22**, the differences could be due to inaccuracies in the predicted binding modes to the “real” configurations. Further studies, including competition binding experiments and protein X-ray crystallography, may give more information about the interactions of these two molecules to Hsp90 MD.

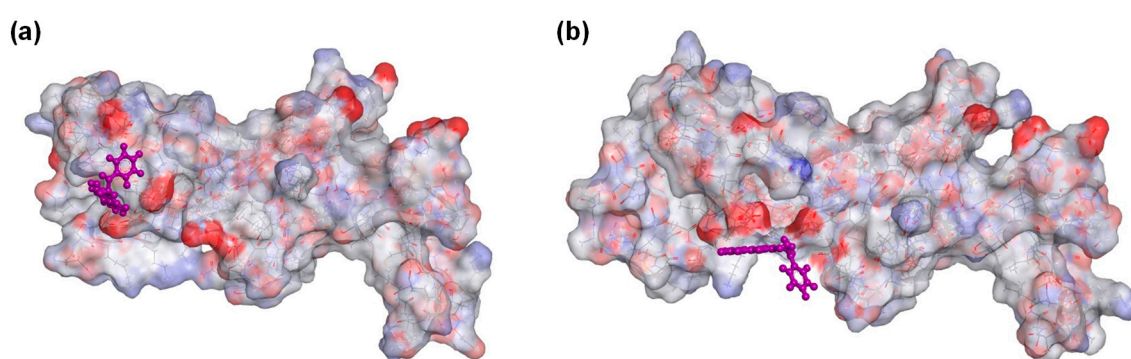


Figure 2. Docking of compound **12** to (a) Hsp90 α MD (PDB ID: 3Q6M) binding pocket (10 Å around Glu-375) and to (b) Hsp90 β MD (PDB id: 3PRY) binding pocket (10 Å around Asp-367). For aesthetic reason, residues 359–492 and 350–484 were shown for Hsp90 α and Hsp90 β , respectively. Both of the displays were processed from the ligand poses as predicted by the GoldScore (GS) scoring function.

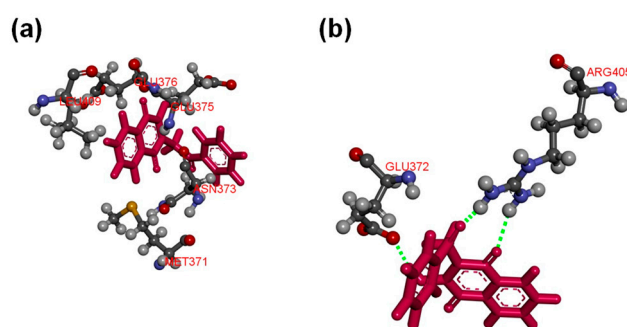


Figure 3. (a) Compound **12** does not form any hydrogen bonding interactions with the neighbouring amino acid residues of Hsp90 α MD (PDB ID: 3Q6M) at the binding pocket (10 Å around Glu-375); (b) compound **12** forms hydrogen bonds with residues Glu-372 and Arg-405 of Hsp90 β MD (PDB id: 3PRY) at the binding pocket (10 Å around Asp-367). Both of the displays were processed from the ligand poses as predicted by the GS scoring function.

To check for the compatibility of the ligands with biological systems, their physicochemical properties were derived. The calculated molecular descriptors for the eight derivatives were molecular weight (MW), lipophilicity (logP), number of hydrogen bond donor (HD), number of hydrogen bond acceptor (HA), polar surface area (PSA), and number of rotatable bonds (RB), and are displayed in Table 2. For MW, the values span from lead-like, through drug-like space to known drug space (KDS; see Table 3 for definitions) [76–78]. HD for most compounds fit within the lead-like space [76,77]. The log P values lie in the range of 0.8 and 4.3 and the PSA values range from 91.2 to 153.9, with the latter reaching into KDS [78].

The Known Drug Indexes 2a and 2b (KDI_{2a/2b}) [79] were also derived. The KDI reflect the overall balance of the molecular properties of ligands based on KDS. KDI_{2a} is additive with a maximum of 6.0 and for KDI_{2b} the indexes are multiplied giving 1.0 as its maximum. The average for KDI_{2a} for known drugs is 4.08 (\pm 1.27) and the ligands lie in the range of 3.63 to 5.68, i.e., they are well balanced compared to known drugs, except for ligand **17**, which has a large MW resulting in a low index. The KDI_{2b} gives a range of 0.02 to 0.70 with the average of know drugs being 0.18 (\pm 0.20), with ligands **12** and **22** with excellent values of 0.70. In general, the ligands are well balanced, with the notable exception of **17**, and can therefore be considered excellent starting points for further development.

Table 2. Molecular descriptors of the hit compounds.

Compound	MW	HD	HA	Log P	PSA	RB	KDI _{2a/b}
5	409.4	1.25	7	3.3	127.0	8	5.48/0.57
8	445.4	0.25	6.5	4.3	137.3	6	5.27/0.45
9	423.5	1.25	7	3.7	122.5	8	5.46/0.56
10	447.5	2	8.3	3.8	73.9	7	5.54/0.61
12	292.3	1	6.75	1.3	93.2	4	5.66/0.70
17	527.5	4	14.05	0.8	154.0	8	3.63/0.02
22	359.4	1.25	6	3.8	91.2	8	5.68/0.70
24	488.5	3	6.5	3.4	95.6	7	5.48/0.57

3. Materials and Methods

3.1. Recombinant Production of Hsp90 α/β MD

Plasmids pET-21a encoding Hsp90 α/β MD were purchased from GenScript (Central, Hong Kong. For sequence, see Tables S3 and S4), which were then transformed into *Escherichia coli* BL21 (DE3) for protein production. In brief, cells were first grown in 2-YT media to an optical density at 600 nm wavelength (OD₆₀₀) of around 0.6 to 0.8. Protein production was then induced by the addition of 0.2 mM isopropyl-1-thio-D-galactopyranoside (IPTG), which was then further incubated at

15 °C overnight. The harvested cells were resuspended in 25 mM Tris (pH 8.0) supplemented with Protease Inhibitor Cocktail (Abcam, Melbourne, Australia), 5 mM dithiothreitol (DTT), and 2 mM ethylenediaminetetraacetic acid (EDTA). The resuspended cells were lysed by sonication. The filtered cell lysate was applied to 1 mL HiTrap Q FF anion exchange chromatography column (GE Healthcare Life Sciences, Auckland, New Zealand) equilibrated with 25 mM Tris (pH 8.0), 2 mM EDTA, and 2 mM DTT. The protein was eluted with a linear gradient to 1 M NaCl from 0% to 100% over 70 min at a flow rate of 1 mL min⁻¹. The protein was further purified by HiPrep 16/60 Sephacryl S-100 HR gel filtration column (GE Healthcare Life Sciences, Auckland, New Zealand) in 20 mM Tris (pH 7.5), 0.2 M KCl, 2 mM EDTA, and 2 mM DTT. The protein was then concentrated using Amicon Ultra-4 10K centrifugal filter (Merck Millipore, Auckland, New Zealand) and stored at -80 °C until use.

3.2. Molecular Docking

A blind docking of gambogic acid was conducted over the entire MD of Hsp90 β and a binding pocket within a region consisted of residues 350 to 436 was identified. In order to validate the binding site as reported, gambogic acid was docked to the crystal structure of the MD of human Hsp90 β (PDB id: 3PRY, resolution 2.28 Å) which was acquired from the Protein Data Bank (PDB) [80]. GS, CS, ChemPLP, and ASP scoring functions were used to validate the predicted binding modes and relative energies of the ligands using the GOLD v5.4 software suite. The Scigress Ultra v2.6 program (Version FJ 2.6 (EU 3.1.7), Fujitsu Limited, Wellington, New Zealand) was used to prepare the crystal structure as a docking scaffold, by adding hydrogen atoms and removing crystallographic water molecules. The basic amino acids lysine and arginine were defined as protonated. Furthermore, aspartic and glutamic acids were assumed deprotonated. The Scigress software suite was also used for structural optimization of the ligands via MM2 force field method [81]. Scores and root-mean-square deviation (RMSD) between the predicted ligand conformation of the scoring functions were compared to define the centre of binding pocket.

3.3. Pilot Screening

GOLD v5.4 software suite was used for virtual screening. Full experimental details were reported in Section 2.

3.4. Calculation of Molecular Descriptors

QikProp 3.2 software package (Schrödinger, New York, NY, USA) was used to calculate the molecular descriptors, which are the numerical values that assesses the properties of the compounds. The criterion of lead-like, drug-like, and KDS are listed in terms of the six respective molecular descriptors in Table 3 [76–78]. The reliability of QikProp is established for the calculated descriptors [82].

Table 3. Definition of lead-like, drug-like, and known drug space (KDS). The values given are the maximum value for each descriptor.

Molecular Descriptors	Lead-Like Space	Drug-Like Space	Known Drug Space
MW (g·mol ⁻¹)	300	500	800
Log <i>p</i>	3	5	6.5
HD	3	5	7
HA	3	10	15
PSA (Å ²)	60	140	180
RB	3	10	17

3.5. Intrinsic Tryptophan Fluorescence Spectroscopy

Fluorescence was measured using EnSpire Multimode Plate Reader (PerkinElmer, Melbourne, Australia). Experiments were performed in 20 μ M of Hsp90 MD in 20 mM Tris (pH 7.5) and 0.2 M KCl. Different concentration of the virtual hits (InterBioScreen, Bar, Montenegro) or gambogic acid were

added to the mixture. Excitation wavelength was 280 nm and intrinsic fluorescence was measured between 300 and 450 nm. The control experiment with Hsp90 MD on its own was conducted. Background fluorescence arising from the compound was subtracted to generate the final spectrum. The total volume per well of the 96-well microplate was 30 μ L. Non-linear curve fitting of Equation (1) to the data was conducted using SigmaPlot 14.0 (Systat Software, San Jose, CA, USA). All tests were conducted in triplicate and the errors shown are standard deviation. K_D was calculated for each binder using Equation (1), where Δ_{obs} is the changes in fluorescence intensity from the titrations, Δ_{max} is the maximum fluorescence intensity change, $[L_T]$ represents the titrated ligand concentration, and $[P_T]$ indicates the protein concentration.

$$\Delta_{\text{obs}} = \Delta_{\text{max}} \times \frac{(K_D + [L_T] + [P_T]) - \sqrt{(K_D + [L_T] + [P_T])^2 - (4 \times [P_T] \times [L_T])}}{2 \times [P_T]} \quad (1)$$

4. Conclusions

Overall, by using an approach that combines both virtual screening and binding studies, we have successfully identified novel ligands that are selective for the β -isoform of Hsp90 MD. Molecular modelling was used to predict the most probable binding modes of the compounds to Hsp90 MD and intrinsic protein fluorescence was used to measure the binding affinity of our compounds to both isoforms of Hsp90 MD. Although the binding affinity and selectivity of the ligands for the β -isoform appears to be modest (low μ M K_D values, \sim 5 to 7-fold for the best compounds), this is on par with a previous study that reported selective Hsp90 β MD inhibitor (gambogic acid, low μ M K_D value, and \sim 7-fold preference in terms of K_D) [55]. In addition, in a recent study by Khandelwal et al., who reported selective inhibitors for Hsp90 β NTD, their initial hits only showed 2–4-fold selectivity [62]. As all of our compounds fit into the known-drug space, drug-like space, or lead-like space areas, we believe our compounds are therefore good starting points for further developments of more selective Hsp90 β MD inhibitors.

Supplementary Materials: Supplementary materials can be found at <http://www.mdpi.com/1422-0067/20/21/5333/s1>.

Author Contributions: O.W.M. conceived and designed the study, performed the experiments, analysed the data, wrote the paper with the input of all the authors, and reviewed the manuscript. R.C. performed the experiments under the guidance of O.W.M. J.R. conceived and designed the study, analysed the data, and reviewed the manuscript. I.K.H.L. conceived and designed the study, analysed the data, wrote the paper with the input of all authors, and reviewed the manuscript.

Funding: Oi Wei Mak is supported by a University of Auckland Doctoral Scholarship. We thank the University of Auckland for funding.

Acknowledgments: We thank K. Boxen for the DNA sequencing service.

Conflicts of Interest: Jóhannes Reynisson is on the inventors' list for Luminespib, a Hsp90 inhibitor in clinical trials. All other authors declare no conflict of interest.

Abbreviations

ASP	Astex Statistical Potential
ATP	Adenosine triphosphate
ChemPLP	Piecewise Linear Potential
CS	ChemScore
CTD	C-terminal domain
DTT	Dithiothreitol
EDTA	Ethylenediaminetetraacetic acid
GA	Genetic algorithm
GS	GoldScore
HA	Number of hydrogen bond acceptor
HD	Number of hydrogen bond donor
Hsp90	Heat shock protein 90
IPTG	Isopropyl-1-thio-D-galactopyranoside
K_D	Dissociation constant
KDI	Known drug index
KDS	Known drug space
Log P	Lipophilicity
MD	Middle domain
MW	Molecular weight
NTD	N-terminal domain
OD ₆₀₀	Optical density at 600 nm wavelength
PDB	Protein data bank
PSA	Polar surface area
RB	Number of rotatable bonds
RMSD	Root-mean-square deviation

References

- Hickey, E.; Brandon, S.; Smale, G.; Lloyd, D.; Weber, L. Sequence and regulation of a gene encoding a human 89-kilodalton heat shock protein. *Mol. Cell. Biol.* **1989**, *9*, 2615–2626. [[CrossRef](#)]
- Aligue, R.; Akhavan-Niak, H.; Russell, P. A role for Hsp90 in cell cycle control: Wee1 tyrosine kinase activity requires interaction with Hsp90. *EMBO J.* **1994**, *13*, 6099–6106. [[CrossRef](#)]
- Bose, S.; Weikl, T.; Bügl, H.; Buchner, J. Chaperone function of Hsp90-associated proteins. *Science* **1996**, *274*, 1715–1717. [[CrossRef](#)]
- Pearl, L.H.; Prodromou, C. Structure and in vivo function of Hsp90. *Curr. Opin. Struct. Biol.* **2000**, *10*, 46–51. [[CrossRef](#)]
- Burrows, F.; Zhang, H.; Kamal, A. Hsp90 activation and cell cycle regulation. *Cell Cycle* **2004**, *3*, 1530–1536. [[CrossRef](#)]
- Pearl, L.H.; Prodromou, C. Structure and mechanism of the Hsp90 molecular chaperone machinery. *Annu. Rev. Biochem.* **2006**, *75*, 271–294. [[CrossRef](#)]
- Taipale, M.; Jarosz, D.F.; Lindquist, S. HSP90 at the hub of protein homeostasis: Emerging mechanistic insights. *Nat. Rev. Mol. Cell Biol.* **2010**, *11*, 515–528. [[CrossRef](#)]
- Prodromou, C. The ‘active life’ of Hsp90 complexes. *Biochim. Biophys. Acta* **2012**, *1823*, 614–623. [[CrossRef](#)]
- Li, J.; Buchner, J. Structure, function and regulation of the Hsp90 machinery. *Biomed. J.* **2013**, *36*, 106–117.
- Hoter, A.; El-Sabban, M.E.; Naim, H.Y. The HSP90 family: Structure, regulation, function, and implications in health and disease. *Int. J. Mol. Sci.* **2018**, *19*, 2560. [[CrossRef](#)]
- Biebl, M.M.; Buchner, J. Structure, function, and regulation of the Hsp90 machinery. *Cold Spring Harb. Perspect. Biol.* **2019**, a034017. [[CrossRef](#)] [[PubMed](#)]
- Gupta, R.S. Phylogenetic analysis of the 90 kD heat shock family of protein sequences and an examination of the relationship among animals, plants, and fungi species. *Mol. Biol. Evol.* **1995**, *12*, 1063–1073. [[PubMed](#)]
- Chen, B.; Zhong, D.; Monteiro, A. Comparative genomics and evolution of the HSP90 family of genes across all kingdoms of organisms. *BMC Genom.* **2006**, *7*, 156.

14. Johnson, J.L. Evolution and function of diverse Hsp90 homologs and cochaperone proteins. *Biochim. Biophys. Acta* **2012**, *1823*, 607–613. [[CrossRef](#)]
15. Scheibel, T.; Siegmund, H.; Jaenicke, R.; Ganz, P.; Lilie, H.; Buchner, J. The charged region of Hsp90 modulates the function of the N-terminal domain. *Proc. Natl. Acad. Sci. USA* **1999**, *96*, 1297–1302. [[CrossRef](#)]
16. Siligardi, G.; Hu, B.; Panaretou, B.; Piper, P.W.; Pearl, L.H.; Prodromou, C. Co-chaperone regulation of conformational switching in the Hsp90 ATPase cycle. *J. Biol. Chem.* **2004**, *279*, 51989–51998. [[CrossRef](#)]
17. Meng, X.; Devin, J.; Sullivan, W.P.; Toft, D.; Baulieu, E.E.; Catelli, M.G. Mutational analysis of Hsp90 alpha dimerization and subcellular localization: Dimer disruption does not impede “in vivo” interaction with estrogen receptor. *J. Cell Sci.* **1996**, *109*, 1677–1687.
18. Yamada, S.-I.; Ono, T.; Mizuno, A.; Nemoto, T.K. A hydrophobic segment within the C-terminal domain is essential for both client-binding and dimer formation of the HSP90-family molecular chaperone. *Eur. J. Biochem.* **2003**, *270*, 146–154. [[CrossRef](#)]
19. Meyer, P.; Prodromou, C.; Hu, B.; Vaughan, C.; Roe, S.M.; Panaretou, B.; Piper, P.W.; Pearl, L.H. Structural and functional analysis of the middle segment of hsp90: Implications for ATP hydrolysis and client protein and cochaperone interactions. *Mol. Cell* **2003**, *11*, 647–658. [[CrossRef](#)]
20. Hawle, P.; Siepmann, M.; Harst, A.; Siderius, M.; Reusch, H.P.; Obermann, W.M.J. The middle domain of Hsp90 acts as a discriminator between different types of client proteins. *Mol. Cell Biol.* **2006**, *26*, 8385–8395. [[CrossRef](#)]
21. Zuehlke, A.; Johnson, J.L. Hsp90 and co-chaperones twist the functions of diverse client proteins. *Biopolymers* **2010**, *93*, 211–217. [[CrossRef](#)] [[PubMed](#)]
22. Riggs, D.L.; Cox, M.B.; Cheung-Flynn, J.; Prapapanich, V.; Carrigan, P.E.; Smith, D.F. Functional specificity of co-chaperone interactions with Hsp90 client proteins. *Crit. Rev. Biochem. Mol. Biol.* **2004**, *39*, 279–295. [[CrossRef](#)] [[PubMed](#)]
23. Subbarao Sreedhar, A.; Kalmár, É.; Csermely, P.; Shen, Y.-F. Hsp90 isoforms: Functions, expression and clinical importance. *FEBS Lett.* **2004**, *562*, 11–15. [[CrossRef](#)]
24. Prodromou, C. Mechanisms of Hsp90 regulation. *Biochem. J.* **2016**, *473*, 2439–2452. [[CrossRef](#)]
25. Zhang, S.L.; Yu, J.; Cheng, X.K.; Ding, L.; Heng, F.Y.; Wu, N.H.; Shen, Y.F. Regulation of human hsp90 α gene expression. *FEBS Lett.* **1999**, *444*, 130–135. [[CrossRef](#)]
26. Zuehlke, A.D.; Beebe, K.; Neckers, L.; Prince, T. Regulation and function of the human HSP90AA1 gene. *Gene* **2015**, *570*, 8–16. [[CrossRef](#)]
27. Taherian, A.; Krone, P.H.; Ovsenek, N. A comparison of Hsp90 α and Hsp90 β interactions with cochaperones and substrates. *Biochem. Cell Biol.* **2008**, *86*, 37–45. [[CrossRef](#)]
28. Whitesell, L.; Lindquist, S.L. HSP90 and the chaperoning of cancer. *Nat. Rev. Cancer* **2005**, *5*, 761–772. [[CrossRef](#)]
29. Jaeger, A.M.; Whitesell, L. HSP90: Enabler of cancer adaptation. *Annu. Rev. Cancer Bio.* **2019**, *3*, 275–297. [[CrossRef](#)]
30. Zuo, D.S.; Dai, J.; Bo, A.H.; Fan, J.; Xiao, X.Y. Significance of expression of heat shock protein90 α in human gastric cancer. *World J. Gastroenterol.* **2003**, *9*, 2616–2618. [[CrossRef](#)]
31. Okamoto, J.; Mikami, I.; Tominaga, Y.; Kuchenbecker, K.M.; Lin, Y.C.; Bravo, D.T.; Clement, G.; Yagui-Beltran, A.; Ray, M.R.; Koizumi, K.; et al. Inhibition of Hsp90 leads to cell cycle arrest and apoptosis in human malignant pleural mesothelioma. *J. Thorac. Oncol.* **2008**, *3*, 1089–1095. [[CrossRef](#)] [[PubMed](#)]
32. Jhaveri, K.; Modi, S. HSP90 inhibitors for cancer therapy and overcoming drug resistance. *Adv. Pharmacol.* **2012**, *65*, 471–517. [[PubMed](#)]
33. Lu, X.; Xiao, L.; Wang, L.; Ruden, D.M. Hsp90 inhibitors and drug resistance in cancer: The potential benefits of combination therapies of Hsp90 inhibitors and other anti-cancer drugs. *Biochem. Pharmacol.* **2012**, *83*, 995–1004. [[CrossRef](#)] [[PubMed](#)]
34. Lee, J.; Zhang, L.L.; Wu, W.; Guo, H.; Li, Y.; Sukhanova, M.; Venkataraman, G.; Huang, S.; Zhang, H.; Alikhan, M.; et al. Activation of MYC, a bona fide client of HSP90, contributes to intrinsic ibrutinib resistance in mantle cell lymphoma. *Blood Adv.* **2018**, *2*, 2039–2051. [[CrossRef](#)] [[PubMed](#)]
35. Chiosis, G.; Vilenchik, M.; Kim, J.; Solit, D. Hsp90: The vulnerable chaperone. *Drug Discov. Today* **2004**, *9*, 881–888. [[CrossRef](#)]
36. Drysdale, M.J.; Brough, P.A.; Massey, A.; Jensen, M.R.; Schoepfer, J. Targeting Hsp90 for the treatment of cancer. *Curr. Opin. Drug Discov. Dev.* **2006**, *9*, 483–495.

37. Taldone, T.; Gozman, A.; Maharaj, R.; Chiosis, G. Targeting Hsp90: Small-molecule inhibitors and their clinical development. *Curr. Opin. Pharmacol.* **2008**, *8*, 370–374. [[CrossRef](#)]
38. Mahalingam, D.; Swords, R.; Carew, J.S.; Nawrocki, S.T.; Bhalla, K.; Giles, F.J. Targeting HSP90 for cancer therapy. *Br. J. Cancer* **2009**, *100*, 1523–1529. [[CrossRef](#)]
39. Trepel, J.; Mollapour, M.; Giaccone, G.; Neckers, L. Targeting the dynamic HSP90 complex in cancer. *Nat. Rev. Cancer* **2010**, *10*, 537–549. [[CrossRef](#)]
40. Neckers, L.; Workman, P. Hsp90 molecular chaperone inhibitors: Are we there yet? *Clin. Cancer Res.* **2012**, *18*, 64–76. [[CrossRef](#)]
41. Jhaveri, K.; Taldone, T.; Modi, S.; Chiosis, G. Advances in the clinical development of heat shock protein 90 (Hsp90) inhibitors in cancers. *Biochim. Biophys. Acta* **2012**, *1823*, 742–755. [[CrossRef](#)] [[PubMed](#)]
42. Ho, N.; Li, A.; Li, S.; Zhang, H. Heat shock protein 90 and role of its chemical inhibitors in treatment of hematologic malignancies. *Pharmaceuticals* **2012**, *5*, 779–801. [[CrossRef](#)] [[PubMed](#)]
43. Lu, X.; Luan, W.; Ruden, D. Hsp90 inhibitors and the reduction of anti-cancer drug resistance by non-genetic and genetic mechanisms. *Pharmaceuticals* **2012**, *5*, 890–898. [[CrossRef](#)] [[PubMed](#)]
44. Garcia-Carbonero, R.; Carnero, A.; Paz-Ares, L. Inhibition of HSP90 molecular chaperones: Moving into the clinic. *Lancet Oncol.* **2013**, *14*, e358–e369. [[CrossRef](#)]
45. Bhat, R.; Tummalapalli, S.R.; Rotella, D.P. Progress in the discovery and development of heat shock protein 90 (hsp90) inhibitors. *J. Med. Chem.* **2014**, *57*, 8718–8728. [[CrossRef](#)] [[PubMed](#)]
46. Khandelwal, A.; Crowley, V.M.; Blagg, B.S. Natural product inspired N-terminal Hsp90 inhibitors: From bench to bedside? *Med. Res. Rev.* **2016**, *36*, 92–118. [[CrossRef](#)]
47. Condelli, V.; Crispo, F.; Pietrafesa, M.; Lettini, G.; Matassa, D.S.; Esposito, F.; Landriscina, M.; Maddalena, F. HSP90 molecular chaperones, metabolic rewiring, and epigenetics: Impact on tumor progression and perspective for anticancer therapy. *Cells* **2019**, *8*, 532. [[CrossRef](#)]
48. Whitesell, L.; Cook, P. Stable and specific binding of heat shock protein 90 by geldanamycin disrupts glucocorticoid receptor function in intact cells. *Mol. Endocrinol.* **1996**, *10*, 705–712.
49. Miyata, Y. Hsp90 inhibitor geldanamycin and its derivatives as novel cancer chemotherapeutic agents. *Curr. Pharm. Des.* **2005**, *11*, 1131–1138. [[CrossRef](#)]
50. Usmani, S.Z.; Bona, R.; Li, Z. 17 AAG for HSP90 inhibition in cancer—from bench to bedside. *Curr. Mol. Med.* **2009**, *9*, 654–664. [[CrossRef](#)]
51. Ying, W.; Du, Z.; Sun, L.; Foley, K.P.; Proia, D.A.; Blackman, R.K.; Zhou, D.; Inoue, T.; Tatsuta, N.; Sang, J.; et al. Ganetespib, a unique triazolone-containing Hsp90 inhibitor, exhibits potent antitumor activity and a superior safety profile for cancer therapy. *Mol. Cancer Ther.* **2012**, *11*, 475–484. [[CrossRef](#)] [[PubMed](#)]
52. Lin, S.F.; Lin, J.D.; Hsueh, C.; Chou, T.C.; Yeh, C.N.; Chen, M.H.; Wong, R.J. Efficacy of an HSP90 inhibitor, ganetespib, in preclinical thyroid cancer models. *Oncotarget* **2017**, *8*, 41294–41304. [[CrossRef](#)] [[PubMed](#)]
53. Donnelly, A.; Blagg, B.S. Novobiocin and additional inhibitors of the Hsp90 C-terminal nucleotide-binding pocket. *Curr. Med. Chem.* **2008**, *15*, 2702–2717. [[CrossRef](#)] [[PubMed](#)]
54. Zhang, F.Z.; Ho, D.H.; Wong, R.H. Triptolide, a HSP90 middle domain inhibitor, induces apoptosis in triple manner. *Oncotarget* **2018**, *9*, 22301–22315. [[CrossRef](#)]
55. Yim, K.H.; Prince, T.L.; Qu, S.; Bai, F.; Jennings, P.A.; Onuchic, J.N.; Theodorakis, E.A.; Neckers, L. Gambogic acid identifies an isoform-specific druggable pocket in the middle domain of Hsp90 β . *Proc. Natl. Acad. Sci. USA* **2016**, *113*, E4801–E4809. [[CrossRef](#)]
56. Chan, C.T.; Reeves, R.E.; Geller, R.; Yaghoubi, S.S.; Hoehne, A.; Solow-Cordero, D.E.; Chiosis, G.; Massoud, T.F.; Paulmurugan, R.; Gambhir, S.S. Discovery and validation of small-molecule heat-shock protein 90 inhibitors through multimodality molecular imaging in living subjects. *Proc. Natl. Acad. Sci. USA* **2012**, *109*, E2476–E2485. [[CrossRef](#)]
57. Duerfeldt, A.S.; Peterson, L.B.; Maynard, J.C.; Ng, C.L.; Eletto, D.; Ostrovsky, O.; Shinogle, H.E.; Moore, D.S.; Argon, Y.; Nicchitta, C.V.; et al. Development of a Grp94 inhibitor. *J. Am. Chem. Soc.* **2012**, *134*, 9796–9804. [[CrossRef](#)]
58. Hughes, P.F.; Barrott, J.J.; Carlson, D.A.; Loiselle, D.R.; Speer, B.L.; Bodoor, K.; Rund, L.A.; Haystead, T.A. A highly selective Hsp90 affinity chromatography resin with a cleavable linker. *Bioorg. Med. Chem.* **2012**, *20*, 3298–3305. [[CrossRef](#)]

59. Ye, B.X.; Deng, X.; Shao, L.D.; Lu, Y.; Xiao, R.; Liu, Y.J.; Jin, Y.; Xie, Y.Y.; Zhao, Y.; Luo, L.F.; et al. Vibsanin B preferentially targets HSP90 β , inhibits interstitial leukocyte migration, and ameliorates experimental autoimmune encephalomyelitis. *J. Immunol.* **2015**, *194*, 4489–4497. [[CrossRef](#)]
60. Liu, W.; Vielhauer, G.A.; Holzbeierlein, J.M.; Zhao, H.; Ghosh, S.; Brown, D.; Lee, E.; Blagg, B.S.J. KU675, a concomitant heat-shock protein inhibitor of Hsp90 and Hsc70 that manifests isoform selectivity for Hsp90 α in prostate cancer cells. *Mol. Pharmacol.* **2015**, *88*, 121–130. [[CrossRef](#)]
61. Stothert, A.R.; Suntharalingam, A.; Tang, X.; Crowley, V.M.; Mishra, S.J.; Webster, J.M.; Nordhues, B.A.; Huard, D.J.E.; Passaglia, C.L.; Lieberman, R.L.; et al. Isoform-selective Hsp90 inhibition rescues model of hereditary open-angle glaucoma. *Sci. Rep.* **2017**, *7*, 17951. [[CrossRef](#)] [[PubMed](#)]
62. Khandelwal, A.; Kent, C.N.; Balch, M.; Peng, S.; Mishra, S.J.; Deng, J.; Day, V.W.; Liu, W.; Subramanian, C.; Cohen, M.; et al. Structure-guided design of an Hsp90 β N-terminal isoform-selective inhibitor. *Nat. Commun.* **2018**, *9*, 425. [[CrossRef](#)] [[PubMed](#)]
63. Neckers, L.; Blagg, B.; Haystead, T.; Trepel, J.B.; Whitesell, L.; Picard, D. Methods to validate Hsp90 inhibitor specificity, to identify off-target effects, and to rethink approaches for further clinical development. *Cell Stress Chaperone* **2018**, *23*, 467–482. [[CrossRef](#)] [[PubMed](#)]
64. Hong, D.S.; Banerji, U.; Tavana, B.; George, G.C.; Aaron, J.; Kurzrock, R. Targeting the molecular chaperone heat shock protein 90 (HSP90): Lessons learned and future directions. *Cancer Treat. Rev.* **2013**, *39*, 375–387. [[CrossRef](#)] [[PubMed](#)]
65. Powers, M.V.; Workman, P. Inhibitors of the heat shock response: Biology and pharmacology. *FEBS Lett.* **2007**, *581*, 3758–3769. [[CrossRef](#)] [[PubMed](#)]
66. Huang, R.; Ayine-Tora, D.M.; Muhammad Rosdi, M.N.; Li, Y.; Reynisson, J.; Leung, I.K.H. Virtual screening and biophysical studies lead to HSP90 inhibitors. *Bioorg. Med. Chem. Lett.* **2017**, *27*, 277–281. [[CrossRef](#)] [[PubMed](#)]
67. Hetényi, C.; van der Spoel, D. Efficient docking of peptides to proteins without prior knowledge of the binding site. *Protein Sci.* **2002**, *11*, 1729–1737. [[CrossRef](#)]
68. Hetényi, C.; van der Spoel, D. Blind docking of drug-sized compounds to proteins with up to a thousand residues. *FEBS Lett.* **2006**, *580*, 1447–1450. [[CrossRef](#)]
69. Wang, R.; Wang, S. How does consensus scoring work for virtual library screening? An idealized computer experiment. *J. Chem. Inf. Comput. Sci.* **2001**, *415*, 1422–1426. [[CrossRef](#)]
70. Charifson, P.S.; Corkery, J.J.; Murcko, M.A.; Walters, W.P. Consensus scoring: A method for obtaining improved hit-rates from docking databases of three-dimensional structures into proteins. *J. Med. Chem.* **1999**, *42*, 5100–5109. [[CrossRef](#)]
71. Jones, G.; Willett, P.; Glen, R.C.; Leach, A.R.; Taylor, R. Development and validation of a genetic algorithm for flexible docking. *J. Mol. Biol.* **1997**, *267*, 727–748. [[CrossRef](#)] [[PubMed](#)]
72. Eldridge, M.D.; Murray, C.W.; Auton, T.R.; Paolini, G.V.; Mee, R.P. Empirical scoring functions: I. The development of a fast empirical scoring function to estimate the binding affinity of ligands in receptor complexes. *J. Comput. Aided Mol. Des.* **1997**, *11*, 425–445. [[CrossRef](#)] [[PubMed](#)]
73. Verdonk, M.L.; Cole, J.C.; Hartshorn, M.J.; Murray, C.W.; Taylor, R.D. Improved protein-ligand docking using GOLD. *Proteins* **2003**, *52*, 609–623. [[CrossRef](#)] [[PubMed](#)]
74. Korb, O.; Stutzle, T.; Exner, T.E. Empirical scoring functions for advanced protein-ligand docking with PLANTS. *J. Chem. Inf. Model.* **2009**, *49*, 84–96. [[CrossRef](#)]
75. Mooij, W.; Verdonk, M.L. General and targeted statistical potentials for protein-ligand interactions. *Proteins* **2005**, *61*, 272–287. [[CrossRef](#)]
76. Lipinski, C.A. Lead- and drug-like compounds: The rule-of-five revolution. *Drug Discov. Today Technol.* **2004**, *1*, 337–341. [[CrossRef](#)]
77. Leeson, P.D.; Springthorpe, B. The influence of drug-like concepts on decision-making in medicinal chemistry. *Nat. Rev. Drug Discov.* **2007**, *6*, 881–890. [[CrossRef](#)]
78. Bade, R.; Chan, H.F.; Reynisson, J. Characteristics of known drug space. Natural products, their derivatives and synthetic drugs. *Eur. J. Med. Chem.* **2010**, *45*, 5646–5652. [[CrossRef](#)]
79. Eurtivong, C.; Reynisson, J. The Development of a Weighted Index to Optimise Compound Libraries for High Throughput Screening. *Mol. Inform.* **2019**, *38*, 1800068. [[CrossRef](#)]
80. Berman, H.; Henrick, K.; Nakamura, H. Announcing the worldwide Protein Data Bank. *Nat. Struct. Mol. Biol.* **2003**, *10*, 980. [[CrossRef](#)]

81. Allinger, N.L. Conformational analysis. 130. MM2. A hydrocarbon force field utilizing V1 and V2 torsional terms. *J. Am. Chem. Soc.* **1977**, *99*, 8127–8134. [[CrossRef](#)]
82. Ioakimidis, L.; Thoukydidis, L.; Mirza, A.; Naeem, S.; Reynisson, J. Benchmarking the Reliability of QikProp. Correlation between Experimental and Predicted Values. *QSAR Comb. Sci.* **2008**, *27*, 445–456. [[CrossRef](#)]



© 2019 by the authors. Licensee MDPI, Basel, Switzerland. This article is an open access article distributed under the terms and conditions of the Creative Commons Attribution (CC BY) license (<http://creativecommons.org/licenses/by/4.0/>).